
Deep Learning-Based Multi-Tooth Segmentation on Panoramic Radiographs Using YOLOv8 Architecture

Pramawahyudi¹⁾, Ahmad Ridwan^{2*)}, Desy Purnama Sari³⁾, Hanisah⁴⁾, Yogendra Rao Musunuri⁵⁾

¹⁾ Department Computer Engineering, Faculty of Information Technology, Universitas Andalas, Indonesia,

²⁾ Department of Informatics, Faculty of Computer Science, Universitas AMIKOM Yogyakarta, Indonesia

³⁾ Department of Prosthodontics, Faculty of Dentistry, Universitas Andalas, Indonesia

⁴⁾ Kol. H. M. Syukur Jambi Mental Hospital, Jambi Provincial Government, Jambi, Indonesia

⁵⁾ Department of Control and Instrumentation Engineering, Changwon National University, South Korea

¹⁾pramawahyudi@it.unand.ac.id, ^{2*)}ahmadridwan@amikom.ac.id, ³⁾desypurnamasari@dent.unand.ac.id,

⁴⁾anisaanisajbi.21@gmail.com, ⁵⁾rao@gmail.com

ABSTRACT

This research introduces a multi-class tooth-level segmentation framework on panoramic radiographs using YOLOv8, trained on clinically annotated Indonesian dental data. A dataset of 302 annotated panoramic radiographs from patients at Universitas Andalas Dental Hospital was utilized, with each tooth precisely labeled according to international dental nomenclature. The model was trained using transfer learning with the YOLOv8 variant, optimized with the Adam algorithm, and evaluated using precision, recall, F1-score, and Intersection over Union (IoU). The results demonstrate that YOLOv8 is not only effective for lesion detection but also robust for fine-grained anatomical dental segmentation. The performance achieved 93.72% accuracy, 92.67% precision, 98.88% recall, and 95.58% F1-score, indicating high accuracy in tooth detection and boundary delineation. Qualitative analysis confirmed accurate segmentation across a wide range of anatomical variations, including crowding, impaction, and prosthetics. This research establishes YOLOv8 as a highly effective tool for dental image segmentation, offering significant potential to improve diagnostic efficiency, support odontological forensics, and enable automated patient record management. Future work will focus on integrating multi-class pathology detection and 3D reconstruction.

Keywords: Deep Learning; Dental Panoramic; Radiographs; Segmentation; YOLOv8

INTRODUCTION

Panoramic radiography is one of the most widely used radiographic examinations because it can provide a two-dimensional (2D) image of the teeth and upper jawbone (Kim 2024). Panoramic radiographs are obtained by exposing the patient to X-rays, where the X-ray source and film (digital image receptor) move in opposite directions at the same speed around the patient's head (Alali et al. 2024). Panoramic radiography has the advantage of visualizing a wide area; however, it still presents several problems with panoramic radiographic images, including overlapping structures, distortion, and uneven lighting (Lin et al. 2023)(Machado et al. 2023). This can make it difficult for medical personnel to identify specific body parts, such as organs, tissues, and other anatomical structures.

Image segmentation is a crucial step in image processing and can be applied anywhere when the internal components of an image need to be analyzed (Katsumata 2023)(Feng, Xu, and Wang 2023). The purpose of image segmentation is to separate an object's area from the background area, allowing for easy analysis and identification of objects that require a significant amount of visual perception (Alam et al. 2025)(W. Chen et al. 2024)(Nambiar and Nanjundegowda 2024). Automatic segmentation can be performed using computer algorithms in the identification process. Automatic segmentation is faster and more accurate than manual segmentation because it can perform high data processing and rapid calculations (Isaksson et al. 2023)(Zaidi et al. 2022). Current methods for dental image analysis often rely on traditional image processing techniques such as edge detection or thresholding, which struggle with noise, overlapping structures, and anatomical variability (de Magalhães and Santos 2025)(Ali and Zhang 2024). In recent years, artificial intelligence (AI) and intensive learning have been widely implemented to assist dentists in analyzing patients' teeth (Ding et al. 2023)(X. Chen et al. 2024). With the growing volume of dental imaging data, there is an urgent need for automated, reliable, and scalable solutions to streamline diagnosis and improve consistency

* Corresponding author



[Creative Commons Attribution-NonCommercial-ShareAlike 4.0 International License.](https://creativecommons.org/licenses/by-nc-sa/4.0/)

(Carrillo-Perez et al. 2022)(Dayı et al. 2023).

Several studies related to the application of deep learning for analyzing panoramic images, notably by Karaoglu et al. (2023), have successfully identified teeth in panoramic images using the deep learning method. The results of this experiment show the effectiveness of the proposed method in detecting, segmenting, and numbering panoramic radiographs. The use of deep learning in segmentation has the potential to reduce the workload of dental radiologists, as it can accelerate the diagnosis process and enhance the accuracy of panoramic dental radiography images (Karaoglu et al. 2023). Additionally, research conducted by Sivari et al. (2023) applied deep learning to the diagnosis of dental disease anomalies. The deep learning algorithm showed good performance in evaluating visual data for the diagnosis of dental diseases. The application of deep learning in dental and oral health services enables more comprehensive and accurate image evaluation and disease detection, potentially leading to reduced treatment costs and improved patient outcomes (Sivari et al. 2023).

Furthermore, research conducted by Shon et al. (2022) classified the stages of periodontitis in panoramic dental radiographs using deep learning methods. The results showed that the model had an accuracy of 93%, indicating a high level of performance. This model is expected to reduce misdiagnosis by dental specialists using dental radiographs of patients with periodontitis. This model also enables the treatment and prevention of the disease based on early diagnosis and the determination of the disease progression rate (Shon et al. 2022).

Finally, a study conducted by Rasic et al. (2023) investigated the detection and segmentation of radiolucent lesions in the mandible on panoramic radiographs using YOLOv8. This study utilized 226 panoramic radiograph images, and the results demonstrated an excellent ability to detect and segment radiolucent lesions in the mandible automatically. This model achieved a detection accuracy of 0.918 without augmentation and 0.952 with augmentation, outperforming previous models with smaller datasets (Rašić et al. 2023).

Although several deep learning approaches have been explored, many suffer from poor generalization, limited boundary precision, or limited compatibility with real-world clinical settings. There remains a gap in the development of high-accuracy, real-time end-to-end segmentation systems explicitly designed for panoramic dental images. Although several deep learning approaches have been explored, many suffer from low generalization accuracy, poor boundary accuracy, or incompatibility with real-world clinical settings. There remains a gap in the development of high-accuracy, real-time end-to-end segmentation systems explicitly designed for panoramic dental images. This study seeks to address shortcomings in previous studies that have primarily focused on lesion detection or single-tooth localization. At the same time, robust tooth-level multi-class segmentation on panoramic radiographs remains underexplored, particularly in real-world clinical datasets. This study also uses YOLOv8 for tooth anatomy segmentation and develops a multi-class segmentation model. In addition, this research helps evaluate clinical readiness and automating the archiving of dental charts in general dentistry and forensic medicine, thereby simplifying and increasing efficiency in patient data management.

METHOD

YOLOv8 Architecture

The YOLOv8 architecture is divided into three parts: backbone, neck, and head. The backbone is responsible for extracting patterns, edges, textures, and shapes from the input image. The backbone consists of conv (convolution), SPD-conv (Spatial Pyramid Dilated Convolution), C2f (Cross Stage Partial Connections with Fusion), and SPPF (Spatial Pyramid Pooling-Fast). Conv enables YOLOv8 to detect, recognize, and distinguish objects in images. SPD-conv, C2f, and SPPF serve to enhance the model's ability to capture multiscale features, particularly for small objects (S. Chen et al. 2024). The neck combines several features in the backbone, allowing the network to detect objects more effectively. The neck section consists of upsample, concat, conv, and GAM (Global Attention Mechanism) to improve resolution and preserve features from the backbone. The head section is responsible for final detection, which produces bounding boxes and object classification. The working architecture of YOLOv8 is illustrated in Figure 1.

* Corresponding author



[Creative Commons Attribution-NonCommercial-ShareAlike 4.0 International License.](https://creativecommons.org/licenses/by-nc-sa/4.0/)

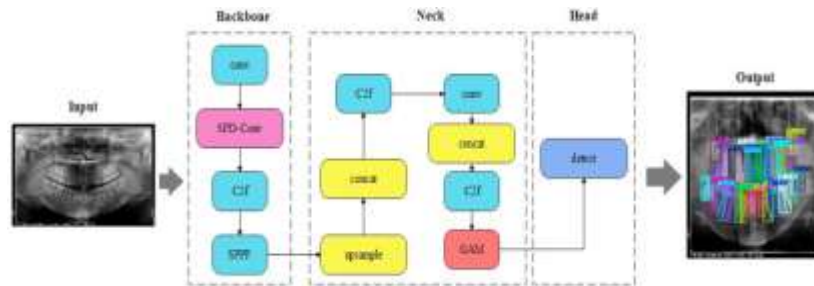


Figure 1. YOLOv8 Architecture

Dataset Acquisition and Annotation

A total of 302 panoramic radiographs were retrospectively collected from adult patients at the Radiology Department of Andalas University Dental and Oral Hospital (RSGM Unand) between June 2024 and July 2025. All images were anonymized and approved in accordance with institutional ethical guidelines. The results of the panoramic radiographic images used in this research are illustrated in Figure 2.

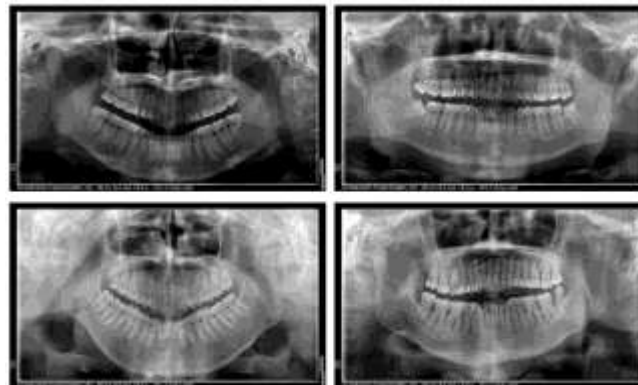


Figure 2. Panoramic Radiographic Image

Each tooth was manually segmented using Roboflow, adhering to the FDI World Dental Federation notation system (ISO 3950). Annotations included all 28–32 permanent teeth, accounting for extractions, implants, crowns, and impacted molars. The dataset was split into training (70%, 211 images), validation (15%, 45 images), and testing sets (15%, 46 images).

Pre-Processing

All images were standardized to 1280×640 pixels to preserve detail. They were then converted to grayscale, a powerful dimensionality reduction strategy when color is not a key feature. Data augmentation techniques applied during training included random rotation ($\pm 10^\circ$), horizontal flipping, brightness and contrast adjustments, and Gaussian noise injection. These measures improved the model's robustness to imaging artifacts and variations in patient position. The model architecture parameters are shown in Table 1.

Table 1. Model architecture hyperparameters

Hyperparameter	Value
Image Size	1280×640
Batch Size	10
Learning Rate	0.01
Epoch	50, 60, 100, 300
Optimizer	ADAM

* Corresponding author



This research varied the number of epochs to obtain the best segmentation results. The number of epochs used varied from 50 to 300. Based on these variations, 300 epochs yielded improvements in evaluation metrics. Epochs of 50, 60, and 100 yielded relatively low evaluation metrics and suboptimal tooth segmentation results. This indicates that too few epochs prevent the model from having enough time to learn the patterns in the teeth in depth. As a result, the model fails to segment teeth accurately. This indicates that a small number of epochs will prevent the model from segmenting optimally, because fewer epochs require less time during training. Therefore, the model does not have enough time to learn the tooth patterns in depth.

Evaluation Metrics

There are several methods to evaluate system performance, namely accuracy, recall, precision, F1 score, and mean Average Precision (mAP). Accuracy is a measure of how often the model makes correct predictions, as shown in Equation 1 (S. Chen et al. 2024). High recall indicates that the class is recognized correctly, as shown in Equation 2 (Lam et al. 2025). Precision is obtained by dividing the total number of correctly classified positive examples by the total number of predicted positive examples, as shown in Equation 3 (Nassiri and Akhloufi 2025).

$$Accuracy = \frac{TP + TN}{TP + TN + FP + FN} \quad (1)$$

$$Recall = \frac{TP}{TP + FN} \quad (2)$$

$$Precision = \frac{TP}{TP + FP} \quad (3)$$

$$F1 - score = 2 \times \frac{Precision \times Recall}{Precision + Recall} \quad (4)$$

Where True Positive (TP) is an actual value that is positive and also predicted to be positive, while True Negative (TN) is an actual value that is negative and also predicted to be negative. A false positive (FP) is an actual value that is negative but predicted to be positive. At the same time, False Negative (FN) is an actual value that is positive but predicted to be negative. A condition where Recall is high and Precision is low means that most positive examples are recognized correctly (low FN), but there are many false positives (high FP). Meanwhile, a condition where Recall is low and Precision is high means that many positive examples are missed (high false negatives, or FN) with few false positives (low false positives, or FP) (Jegham et al. 2025). The F1 score is used as a comparison between the average Precision and Recall, which are weighted according to Equation 4. (Ridwan, Purbolingga, and Hanisah 2024)(Purbolingga, Ridwan, and Putri 2025). In the formula above, TP (True Positive) indicates the total number of correct predictions, which is when the model successfully detects an existing object. FP (False Positive) refers to the total number of incorrect predictions, which is when the model detects an object that does not actually exist, indicating potential overfitting or detection errors. FN (False Negative) refers to the total number of incorrect predictions where the model fails to detect an object that should have been detected but was not detected (Purbolingga et al. 2025).

$$mAP = \frac{1}{N} \sum_{k=0}^{k=n} AP_k \quad (5)$$

$$mAP50 = \frac{1}{N} \sum_{k=0}^{k=n} AP_{50}^k \quad (6)$$

* Corresponding author



[Creative Commons Attribution-NonCommercial-ShareAlike 4.0
International License.](https://creativecommons.org/licenses/by-nc-sa/4.0/)

$$mAP50 = \frac{1}{N} \sum_{k=0}^{k=n} AP_{50-95}^k \tag{7}$$

In the above formula, n is used to represent the total number of classes in the dataset, while k is an index that indicates each class from 0 to n (with n as the last class). The notation AP_k refers to the Average Precision value for class k , and $\Sigma (k = 0 \text{ to } n)$ is used to sum the Average Precision of all classes. mAP is the average precision at various recall levels, used to evaluate the overall performance of the object detection model. mAP can be varied based on the threshold value of IoU (Intersection over Union) obtained from the input data entered into the model. Variations of mAP50 and mAP50-95 are applied nted in Equation (7) (Zhu et al. 2025).

In this section, each researin this study as parameters to assess model performance. mAP50 is the mAP obtained with the IoU threshold set at 0.50. The formula for mean average precision 50 can be seen in Equation (4), while mAP50-95 is calculated with a varying IoU threshold range, starting from 0.50 to 0.95. The formula for mean average precision (50-95) is presecher is expected to be able to make the most recent contribution related to the solution to the existing problems. Researchers can also use images, diagrams, and flowcharts to explain the solutions to these problems.

RESULT

YOLOv8 Model Performance Evaluation Results

The YOLOv8 model generally performed very well, particularly with high segmentation performance across all 32 tooth classes, strong recall, and mAP50, indicating reliable anatomical localization. However, some classes, such as 14, 27, and 36, had lower precision, recall, or mAP values than others. This could be a focus for improvement, for example, by increasing the variety of datasets for these classes or using data augmentation techniques. A graph of the model's evaluation results during training is shown in Figure 3.

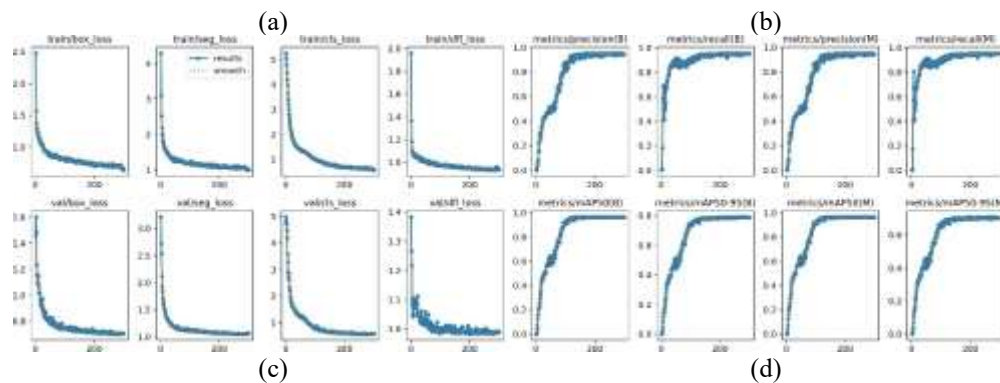


Figure 3. (a) Loss Function Training (b) Validation Loss (c) Evaluation Metrics (d) Mean Average Precision

Based on the image above, all validation losses show a significant decrease, and there are no signs of serious overfitting. The model can learn from well-labeled data, so it does not require early stopping. The image above also shows the model's precision and recall at each epoch. The precision and recall graphs approach 1 as the number of epochs increases, indicating that the model is increasingly accurate at detecting the correct object (precision) and at finding all existing objects (recall). In addition, the mAP graph shows a steady increase as the number of epochs increases. This indicates that the model is increasingly accurate in detecting objects and improving its overall performance.

Based on the YOLOv8 model performance evaluation, it shows good performance across all evaluation metrics, namely accuracy, F1-score, precision, recall, mean Average Precision at an IoU threshold of 50% (mAP50), and average mAP at various IoU thresholds (mAP50-95). The accuracy of YOLOv8 is 93.72%, indicating that, overall, YOLOv8 makes more accurate predictions. This higher accuracy reflects the model's ability to provide more reliable and accurate image classification. The YOLOv8 model's precision is 92.67%. The high precision of YOLOv8 indicates that it is more accurate at predicting positive classes. This means that when YOLOv8 classifies an image as positive,

* Corresponding author



the prediction is most likely correct. The results of the YOLOv8 model performance evaluation are shown in Table 2.

Table 1. Model Evaluation Results

Methods	Accuracy	Precision	Recall	mAP50	mAP50-95	F1-Score
YOLOv8	93,72%	92,67%	98,88%	96,7%	78,2%	95,59%

Figure 4 is a graph showing the relationship between recall (X-axis) and precision (Y-axis). Based on the graph, the mAP (mean Average Precision) value at a threshold of 0.5 is 0.967, which indicates excellent model performance. The graph demonstrates excellent performance, characterized by high precision and recall. The blue line shows the average of all classes, and the gray lines show the individual curves for 32 classes. A high confidence score will result in high precision because the model becomes more selective in making predictions, reducing false positives and thereby decreasing the recall value. This is what causes a significant decline in the graph. Some gray lines appear closer to the thick blue line, indicating that each class has performance close to the model average. However, some lines show greater deviation, indicating an imbalance in the distribution of certain classes. This can occur if there are classes with uneven data distribution or classes that are difficult to detect.

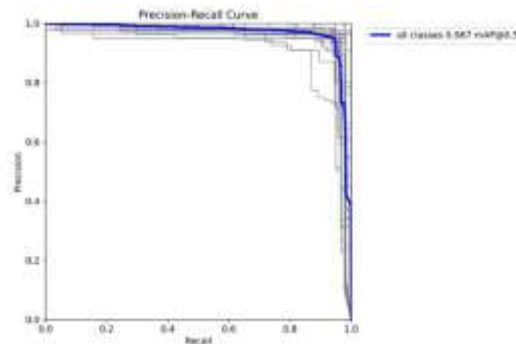


Figure 4. Precision and Recall Relationship Curve

Figure 5 shows the relationship between the confidence score (X-axis) and recall (Y-axis). This graph helps evaluate the model's ability to detect positive cases and observe how changes in the threshold affect recall. The blue line shows the average curve across all classes, with the highest recall of 0.99 at a confidence level of 0.000. The curve remains relatively stable at confidence levels of 0.0 to 0.6, then declines at 0.6, with the sharpest decline occurring at 0.8. As confidence increases, recall decreases sharply because overly high confidence scores make the model excessively selective in its predictions. Only predictions with a high confidence score are considered positive. Consequently, data with low confidence scores are ignored, thereby reducing recall. The gray line represents the recall performance for each class; in general, all lines follow the same pattern. However, some recalls are high at low confidence levels and decrease as confidence increases. This indicates that some classes are more challenging to detect at high confidence levels.

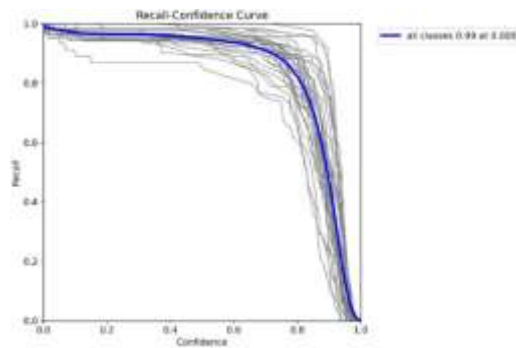


Figure 5. Relationship Curve Between Recall and Confidence Score

Figure 6 illustrates the relationship between the F1-Score value and the confidence score of the YOLOv8 model. The X-axis shows the confidence score, which is the minimum probability that the model considers for predicting a class. At the same time, the Y-axis represents the F1-Score, which combines precision and recall into a single harmonic

* Corresponding author



metric. The thick blue curve shows the average F1-Score value for all classes, with a peak of 0.95 achieved at a confidence score of 0.504. This indicates that this threshold value provides the best balance between precision and recall for the model. The thin gray curve represents the F1-Confidence for each class individually, showing that the model's performance is not entirely uniform for all classes. Some individual curves reach peaks that are lower or higher than the average curve (thick blue). This suggests that certain classes are more challenging for the model to detect or classify than others, even though they generally align with the average curve.

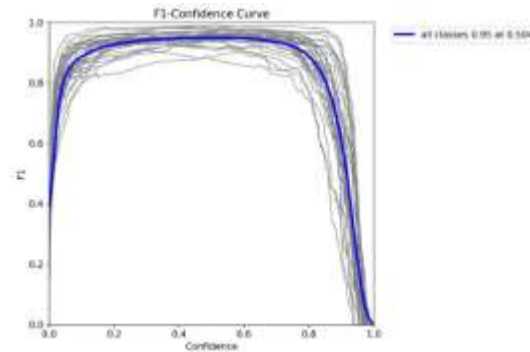


Figure 6. F1-Score Relationship Curve with Confidence Score

Figure 7 shows how the model works in recognizing tooth areas (positive) and non-tooth areas (negative). It was found that the model was able to correctly classify 1,770 positive data points (True Positive) and 620 negative data points (True Negative). However, 140 negative data points were misclassified as positive (False Positive), and 20 positive data points were misclassified as negative (False Negative).

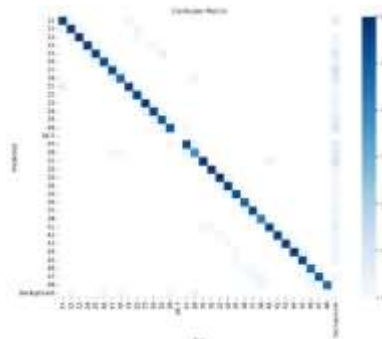


Figure 7. Confusion Matrix

Based on the results of this study, the accuracy, precision, recall, and F1-score percentages were above 90%. These values indicate that the YOLOv8 algorithm can detect objects quickly and accurately, and recognize a wide variety of objects.

Segmentation Results Using YOLOv8

The YOLOv8 segmentation results are shown in Figure 8 as colorful areas. Each tooth will be assigned a bounding box with a label or number according to the tooth nomenclature. Each tooth is also equipped with a confidence score on a scale (value 0-1) that indicates the accuracy level of YOLOv8 for that prediction. The results of several detections have high confidence scores, such as 0.99, suggesting that YOLOv8 successfully detected these teeth with high accuracy, whereas low-confidence scores, such as 0.58, warrant closer inspection. This can occur due to under-segmentation (teeth not fully detected) or over-segmentation (parts that should not be detected as teeth).

* Corresponding author



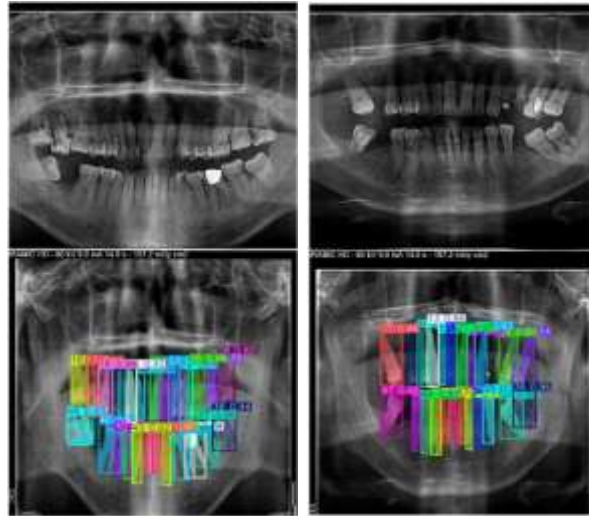


Figure 8. YOLOv8 Segmentation Testing Results

Based on clinical assessments conducted by dentists using Google Forms, the majority rated the model's tooth-numbering results as quite reasonable. The YOLOv8 model accurately identified and marked tooth numbers. However, some results still show overlapping tooth numbers, making some numbers unreadable. It is caused by the close position of teeth, which results in overlapping in automatic numbering. The results of dentists' clinical assessments via Google Forms are shown in Figure 9.

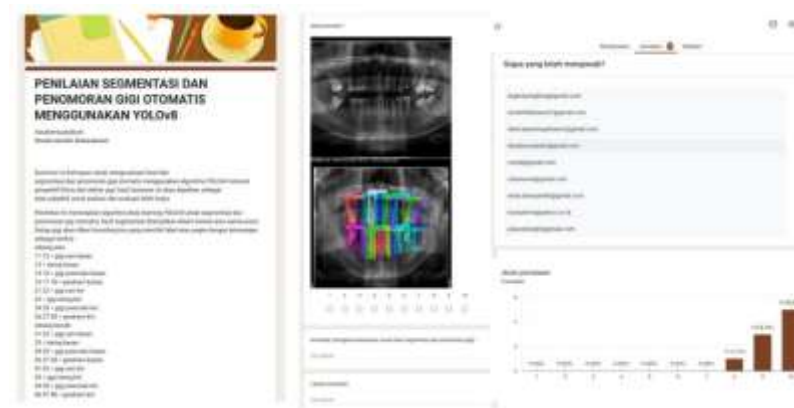


Figure 9. Dentist Clinical Assessment Results

DISCUSSION

The YOLOv8 approach has proven effective due to its ability to achieve an excellent balance between accuracy and efficiency. Some of the technical reasons for this are that the model achieves 93.72% accuracy, 92.67% precision, 98.88% recall, and 95.58% F1-score. Additionally, as a single-stage detector, YOLOv8 makes predictions directly from the entire image in a single pass, making it much faster than manual or traditional segmentation methods. Despite its high accuracy, there are 1.44% false negative cases (teeth not detected). Failures in certain classes were caused by under-segmentation (teeth not fully detected) or over-segmentation (non-tooth parts detected as teeth) in some samples. The model is also set to display only detections with a confidence score above 0.5; teeth with scores below this threshold will not be segmented. Some tooth classes, such as 27 and 36, show lower precision, indicating the need for additional training data specific to these classes to reduce mispredictions.

The results of dental image segmentation research using YOLOv8 can have a direct impact on dental practice, such as reducing the workload of medical personnel because the identification and segmentation processes are carried out automatically and quickly, facilitating the automatic archiving of dental charts, which is very useful for both

* Corresponding author



[Creative Commons Attribution-NonCommercial-ShareAlike 4.0 International License.](https://creativecommons.org/licenses/by-nc-sa/4.0/)

general dentistry and forensic purposes in patient data management, and can reduce the variability of results between operators (subjectivity) that often occurs in manual segmentation. This research can also make a significant scientific contribution in the field of dental imaging, such as proving that deep learning can automatically recognize and classify teeth based on standard nomenclature, even though the images are highly complex, showing that AI technology can overcome traditional obstacles in panoramic images, such as uneven lighting and distortion, to produce more accurate analyses and lay the foundation for the development of future intelligent systems that can assist in early diagnosis and more precise monitoring of oral health development.

CONCLUSION

This research demonstrated that the YOLOv8 algorithm can be effectively applied to automate panoramic dental image segmentation, achieving a very high accuracy of 93.72%. Its main contribution is the development of a system capable of automatically identifying and numbering teeth in accordance with international standards. This transforms the process of creating dental charts, which was previously manual and subjective, into a fast, objective, and efficient digital process, thereby greatly assisting medical personnel in patient data management and dental forensics. Although it performs very well overall, this research still faces technical challenges under specific conditions. The main limitation is segmentation errors (under-segmentation or over-segmentation) in highly complex tooth structures or overlapping objects. Additionally, the false negative rate is 1.44%, as the model fails to detect certain teeth when confidence scores fall below the threshold (0.5), often due to image quality or extreme anatomical variations in specific samples. In terms of future development, this research provides a scientific basis for several strategic steps, including adding datasets covering various pathological conditions (such as caries, impacted teeth, or the use of implants/braces) to improve model generalization. Then, it is necessary to develop more sophisticated image filtering techniques before the training process to reduce noise and enhance contrast in crowded tooth areas. Finally, it is required to conduct trials integrating the model into real-time clinical management software to validate its practical usefulness in dentists' daily operational scenarios.

REFERENCES

- Alali, Y., W. A. Mohammed, A. F. Aldrees, A. M. Alshamrani, M. A. Alabdullatif, and S. A. Alhajri. 2024. "Comparative Efficacy of Digital Panoramic Radiograph and Cone Beam Computed Tomography in Locating Mandibular Foramen." *European Review for Medical and Pharmacological Sciences* 28(8):2996–3005. doi: 10.26355/eurrev_202404_36012.
- Alam, Salem Shamsul, Abdul Ahad, Saif Ahmed, James Dudley, and Taseef Hasan Farook. 2025. "Using Deep Learning to Segment Impacted Molar Teeth from Panoramic Radiographs." *Digital Dentistry Journal* 1(1):100007. doi: <https://doi.org/10.1016/j.ddj.2025.100007>.
- Ali, Momina Liaqat, and Zhou Zhang. 2024. "The YOLO Framework: A Comprehensive Review of Evolution, Applications, and Benchmarks in Object Detection." *Computers* 13(12). doi: 10.3390/computers13120336.
- Carrillo-Perez, Francisco, Oscar E. Pecho, Morales Juan Carlos, Rade D. Paravina, Alvaro Della Bona, Ghinea Razvan, Rosa Pulgar, Pérez María del Mar, and Luis Javier Herrera. 2022. "Applications of Artificial Intelligence in Dentistry: A Comprehensive Review." *Journal of Esthetic and Restorative Dentistry* 34:259–280. doi: 10.1111/jerd.12844.
- Chen, Siyu, Yixuan Li, Yidong Zhang, Yifan Yang, and Xiangxue Zhang. 2024. "Soft X-Ray Image Recognition and Classification of Maize Seed Cracks Based on Image Enhancement and Optimized YOLOv8 Model." *Computers and Electronics in Agriculture* 216:108475. doi: <https://doi.org/10.1016/j.compag.2023.108475>.
- Chen, Wei, Monisha Dhawan, Jonathan Liu, Damie Ing, Kruti Mehta, Daniel Tran, Daniel Lawrence, Max Ganhewa, and Nicola Cirillo. 2024. "Mapping the Use of Artificial Intelligence–Based Image Analysis for Clinical Decision-Making in Dentistry: A Scoping Review." *Clinical and Experimental Dental Research* 10(6). doi: 10.1002/cre2.70035.
- Chen, Xiaokang, Nan Ma, Tongkai Xu, and Cheng Xu. 2024. "Deep Learning-Based Tooth Segmentation Methods in Medical Imaging: A Review." *Proceedings of the Institution of Mechanical Engineers, Part H: Journal of Engineering in Medicine* 238(2):115–31. doi: 10.1177/09544119231217603.
- Dayı, Burak, Hüseyin Üzen, İpek Balıkcı Çiçek, and Şuayip Burak Duman. 2023. "A Novel Deep Learning-Based Approach for Segmentation of Different Type Caries Lesions on Panoramic Radiographs." *Diagnostics* 13(2). doi: 10.3390/diagnostics13020202.

* Corresponding author



[Creative Commons Attribution-NonCommercial-ShareAlike 4.0 International License.](https://creativecommons.org/licenses/by-nc-sa/4.0/)

- Ding, Hao, Jiamin Wu, Wuyuan Zhao, Jukka P. Matinlinna, Michael F. Burrow, and James K. H. Tsoi. 2023. "Artificial Intelligence in Dentistry: A Review." *Frontiers in Dental Medicine* 4(February):1–13. doi: 10.3389/fdmed.2023.1085251.
- Feng, Qihan, Xinzhen Xu, and Zhixiao Wang. 2023. "Deep Learning-Based Small Object Detection: A Survey." *Mathematical Biosciences and Engineering* 20(4):6551–90. doi: 10.3934/mbe.2023282.
- Isaksson, Lars Johannes, Matteo Pepa, Paul Summers, Mattia Zaffaroni, Maria Giulia Vincini, Giulia Corrao, Giovanni Carlo Mazzola, Marco Rotondi, Giuliana Lo Presti, Sara Raimondi, Sara Gandini, Stefania Volpe, Zaharudin Haron, Sarah Alessi, Paola Pricolo, Francesco Alessandro Mistretta, Stefano Luzzago, Federica Cattani, Gennaro Musi, Ottavio De Cobelli, Marta Cremonesi, Roberto Orecchia, Giulia Marvaso, Giuseppe Petralia, and Barbara Alicja Jereczek-Fossa. 2023. "Comparison of Automated Segmentation Techniques for Magnetic Resonance Images of the Prostate." *BMC Medical Imaging* 23(1):1–16. doi: 10.1186/s12880-023-00974-y.
- Jegham, Nidhal, Chan Young Koh, Marwan Abdelatti, and Abdeltawab Hendawi. 2025. "YOLO Evolution: A Comprehensive Benchmark and Architectural Review of YOLOv12, YOLO11, and Their Previous Versions." *Image and Computer Vision* 1–33.
- Karaoglu, Ahmet, Caner Ozcan, Adem Pekince, and Yasin Yasa. 2023. "Numbering Teeth in Panoramic Images: A Novel Method Based on Deep Learning and Heuristic Algorithm." *Engineering Science and Technology, an International Journal* 37:101316. doi: 10.1016/j.jestech.2022.101316.
- Katsumata, Akitoshi. 2023. "Deep Learning and Artificial Intelligence in Dental Diagnostic Imaging." *Japanese Dental Science Review* 59(September):329–33. doi: 10.1016/j.jdsr.2023.09.004.
- Kim, Hyuntae. 2024. "Deep Learning in Dental Radiographic Imaging." *The Journal of the Korean Academy of Pediatric Dentistry* 51(1):1–10. doi: 10.5933/jkapd.2024.51.1.1.
- Lam, Quang Tuan, Minh Huu Nhat Le, I. Ta Lee, and Nguyen Quoc Khanh Le. 2025. "Evaluating YOLO for Dental Caries Diagnosis: A Systematic Review and Meta-Analysis." *Evidence-Based Dentistry*. doi: 10.1038/s41432-025-01180-1.
- Lin, Songyue, Xuejiang Hao, Yan Liu, Dong Yan, Jianwei Liu, and Mingjun Zhong. 2023. "Lightweight Deep Learning Methods for Panoramic Dental X-Ray Image Segmentation." *Neural Computing and Applications* 35(11):8295–8306. doi: 10.1007/s00521-022-08102-7.
- Machado, Leonardo Ferreira, Plauto Christopher Aranha Watanabe, Giovanni Antonio Rodrigues, and Luiz Otavio Murta Junior. 2023. "Deep Learning for Automatic Mandible Segmentation on Dental Panoramic X-Ray Images." *Biomedical Physics & Engineering Express* 9(3):35015. doi: 10.1088/2057-1976/acb7f6.
- de Magalhães, Ana Amélia, and Ana Teresa Santos. 2025. "Applications of Artificial Intelligence in Dentistry: A Comprehensive Review." *Journal of Clinical Medicine* 14(4):1–16. doi: 10.3390/jcm14041277.
- Nambiar, Rajashree, and Raghu Nanjundegowda. 2024. "A Comprehensive Review of AI and Deep Learning Applications in Dentistry: From Image Segmentation to Treatment Planning." *Journal of Robotics and Control (JRC)* 5(6):1744–52. doi: 10.18196/jrc.v5i6.23056.
- Nassiri, Khalid, and Moulay A. Akhloufi. 2025. "YOLO-Based Panoramic Dental X-Ray Image Analysis." *Neural Computing and Applications*. doi: 10.1007/s00521-025-11462-5.
- Purbolingga, Yoan, Ahmad Ridwan, and Dila Marta Putri. 2025. "A Machine Learning-Based Ambiguous Alphabet Recognition for Indonesian Sign Language System (SIBI)." *CogITo Smart Journal* 11(1):1–14. doi: 10.31154/cogito.v11i1.816.1-14.
- Rašić, Mario, Mario Tropčić, Pjetra Karlović, Dragana Gabrić, Marko Subašić, and Predrag Knežević. 2023. "Detection and Segmentation of Radiolucent Lesions in the Lower Jaw on Panoramic Radiographs Using Deep Neural Networks." *Medicina (Lithuania)* 59(12). doi: 10.3390/medicina59122138.
- Ridwan, Ahmad, Yoan Purbolingga, and Hanisah Hanisah. 2024. "Utilizing Convolutional Neural Network for Learning Web-Based Braille Letter Classification System." *Journal of Computer Networks, Architecture and High Performance Computing* 6(1). doi: 10.47709/cnabc.v6i1.3386.
- Shon, Ho Sun, Vungsovanreach Kong, Jae Sung Park, Wooyeong Jang, Eun Jong Cha, Sang Yup Kim, Eun Young Lee, Tae Geon Kang, and Kyung Ah Kim. 2022. "Deep Learning Model for Classifying Periodontitis Stages on Dental Panoramic Radiography." *Applied Sciences (Switzerland)* 12(17). doi: 10.3390/app12178500.
- Sivari, Esra, Guler Burcu Senirkentli, Erkan Bostanci, Mehmet Serdar Guzel, Koray Acici, and Tunc Asuroglu. 2023. "Deep Learning in Diagnosis of Dental Anomalies and Diseases: A Systematic Review." *Diagnostics* 13(15):1–

* Corresponding author



[Creative Commons Attribution-NonCommercial-ShareAlike 4.0 International License.](https://creativecommons.org/licenses/by-nc-sa/4.0/)

28. doi: 10.3390/diagnostics13152512.

Zaidi, Syed Sahil Abbas, Mohammad Samar Ansari, Asra Aslam, Nadia Kanwal, Mamoona Asghar, and Brian Lee. 2022. "A Survey of Modern Deep Learning Based Object Detection Models." *Digital Signal Processing* 126:103514. doi: <https://doi.org/10.1016/j.dsp.2022.103514>.

Zhu, Lei, Wenzhe Gu, Chengyong Liu, Beiyan Zhang, Wentao Liu, and Chaofeng Yuan. 2025. "Image Segmentation Algorithm Based on Improved YOLOv8 Model and Its Application in Underground Coal and Gangue Recognition." *PLoS ONE* 20(5 May):1–21. doi: 10.1371/journal.pone.0321249.

* Corresponding author



[Creative Commons Attribution-NonCommercial-ShareAlike 4.0
International License.](https://creativecommons.org/licenses/by-nc-sa/4.0/)